Journal of Thermal Engineering, Vol. 3, No. 2, pp. 1181-1195 April, 2017, Manuscript Received 29 December 2015, Accepted 27 February 2016, Yildiz Technical University Press, Istanbul, Turkey

EXPERIMENTAL VALIDATION OF LMTD METHOD FOR MICROSCALE HEAT TRANSFER

Nezaket Parlak[1,*], Mesut Gür[2], Tahsin Engin[1], Hasan Küçük[1]

Keywords: Microscale flow and heat transfer, LMTD method, Scaling effects.

ABSTRACT

The single phase fluid flow and heat transfer characteristic has been investigated experimentally. Experiments were conducted to cover transition zone for the Reynolds numbers ranging from 100 to 4800 by fused silica and stainless steel microtubes having diameters of 103-180 μm. The applicability of the Logarithmic Mean Temperature Difference (LMTD) method was revealed and an experimental method was developed to calculate the heat transfer coefficient. Moreover the scaling effects in micro scale such as axial conduction, viscous heating and entrance effects were discussed. The heat transfer coefficients were compared with data obtained by the correlations available in the literature in the study. The Nusselt numbers of microtube flows do not accord with the conventional results when the Reynolds number was lower than 1000. After that, the Nusselt number approaches the conventional theory prediction. On the aspect of fluid characteristics, the friction factor was well predicted with conventional theory and the conventional friction prediction was valid for water flow through microtube with a relative surface roughness less than about 4 %.

INTRODUCTION

Microscale single-phase heat transfer is widely used in a variety of industrial and scientific applications. Examples include biomedical engineering, cellular biology and physical sciences, Micro-Electro-Mechanical Systems (MEMS), micro-satellites, thermal control of electronic devices and micropower generation and other micro fluidic devices (MFD). Kandlikar et al. [1] pointed out proper understanding of fluid flow and heat transfer in these microscale systems was essential for their design and operation in their book. Especially, advances in biomedical and genetic engineering require controlled fluid transport and its precise thermal control in passages with dimensions of several micrometers. In the last decade, a number of researchers have reported the heat transfer and pressure drop data for laminar liquid or gas flow in microchannels. Experimental studies with circular (Adams et al. [2]; Yu et al. [3]; Celata et al. [4]; Tso and Mahulikar [5]; Lelea et al. [6]; Celata et al., [7]; Li et al.,[8]; Zhigang et al. [9], Parlak et al. [10] and [11]), rectangular (Wang and Peng [12], Peng and Peterson [13]; Harms et al. [14]; Gao et al. [15]; Fernando et al. [16]; Lee et al. [17]), trapezoidal (Qu et al. [18]; Wu and Cheng [19]) and triangular (Tiselj et al. [20]) microchannels have been conducted. Accordingly, various reasons have been proposed to explain the anomalous behavior of the transport mechanisms through microchannels such as rarefaction and compressibility effects, viscous dissipation effects, electro-osmotic effects (EDL), property variation effects, channel surface conditions (relative roughness) and experimental uncertainties have been analyzed. The effect of viscous dissipation has an important role in laminar heat transfer, and fluid flow has been investigated by Tso and Mahulikar [5]. They carried out theoretical and experimental studies of circular microchannels taking into account the effect of viscous dissipation by means of the Brinkman number $Br = \mu V^2/k\Delta T$. It is the ratio of the heat production due to viscous forces to heat transferred from the wall to the fluid. Authors underlined that the effect of the Brinkman number was linked to the reduction of the dynamic viscosity between the inlet and the outlet of a microchannel due to the increase in the bulk temperature; this fact could reduce the Brinkman number at the exit by about 50% of its inlet value. Hetsroni et al. [21] have performed the analysis of the single phase heat transfer for circular micro-channels at thermal wall boundary condition T_w = const. with experimental investigations available in the literature. They proposed a correlation between Nu and Br numbers, such

This paper was recommended for publication in revised form by Regional Editor Tolga Taner
1Sakarya University, Faculty of Engineering, Department of Mechanical Engineering, Esentepe Campus Serdivan 54187 Sakarya, Turkey
2İstanbul Technical University, Faculty of Mechanical Engineering, Department of Mechanical Engineering, Gümüşsuyu 34437, İstanbul, Turkey
**E-mail address: naydemir@sakarya.edu.tr*

that $Nu = Nu_0 \mp 8Br$, where Nu_0 is the Nusselt number that corresponds to negligible viscous dissipation. Plus and minus signs correspond to the cooling ($T_0 > T_w$) and heating ($T_0 < T_w$) regimes, respectively. Celata et al. [7] and Parlak et al. [10] have experimentally examined the effect of viscous dissipation in adiabatic microtubes. Their results showed that considerable temperature rises occurred due to viscous dissipation and relatively high pressure losses of flow in experiments with smooth microtubes. They also found a fairly good consistency between the measured and the calculated data from Hagen–Poiseuille equation of laminar flow as long as the viscous heating effects was taken into account in small channels (tube diameter< 100 μm). The ratio between the temperature rise related to the viscous heating and the heat flux at the walls is as a function of the Brinkman number (Br) and Poiseuille number (f Re) as follows;

$$\kappa = \frac{\Delta T_v}{\Delta T_q} = 2BrA^* fRe \qquad (1)$$

where A* is the dimensionless cross-sectional area ($A^* = A/D_h^2$) and the viscous heating can be considered negligible if $\kappa = Br f Re < 0.1$ (Morini [22]). Another scaling effect is the axial heat conduction which is the heat that is conducted axially along a channel wall. It can be neglected for conventional size channels because the wall thickness is usually very small compared to the channel diameter. But microfluidic channels are generally characterized by large $A_s/A_f$and low Peclect number (Pe=RePr), hence the axial conduction tends to become significant. This means that the axial heat conduction should not be neglected. Maranzana et al. [23] proposed a non-dimensional number M, quantifying the part of axial conduction in walls described as follows;

$$M = \frac{\Phi_{cond}}{\Phi_{conv}} = \left(\frac{k_w}{k_f}\frac{D}{L}\frac{A_w}{A_c}\right)\left(\frac{1}{Pe}\right) \qquad (2)$$

and axial conduction can be neglected when M gets lower than 0.01. We found that the values of this number for all experiments carried out in the study were well below the limit of axial conduction. The thermal entry length effects on heat transfer have to be considered in microscale. The entrance effects in tubes become negligible if the follow is satisfied:

$$RePr\frac{D_h}{L} = 10 \qquad (3)$$

The relation $RePr(D_h/L)$ is also known as Graetz number. When Gz number is larger than 10, the thermal entry length effect cannot be ignored. The discrepancies in the results are generally attributed to the roughness effects. For microchannels, the ratio between the geometry of the roughness profile and the hydraulic diameter becomes significantly different from those in conventional channels. For this reason the effect of wall roughness has become important and considerable attention was point on studying heat transfer in microchannels in the past decades. Kandlikar et al. [24] studied the effect of surface roughness in a minichannel flow. They determined that the e/D ratio has a bigger effect in smaller diameter channel than the same e/D ratio in a conventional channel. Kandlikar et al. [25] modelled the surface roughness in rectangular minichannels as saw tooth obstruction. They proposed three new parameters to characterize the surface roughness. The Colebrook's relation for friction factor was modified considering the fact that effective area of flow is decreased when the relative roughness gets larger and hence instead of nominal diameter, the constricted flow diameter is used in their calculations. They modified the Moody diagram according to the calculation of friction factor. The experimental results of local Nusselt number distribution along the axial direction of the stainless steel tubes do not accord with the conventional results when Reynolds number is low and the relative thickness of the tube wall is high. The majority of the scientists have described laminar single phase flow and heat transfer in microchannels by conventional correlations and underlined that scaling effects (entrance effects, conjugate heat transfer, viscous heating, electric double layer (EDL) effects, temperature dependent properties, surface roughness, rarefaction and compressibility effects) should be taken into account. Also, Asadi et al. [26] reported that 76% of the investigators studied heat transfer and pressure drop of single-phase microchannels in the laminar region,

and this showed that the behavior of fluids in the turbulent region remained unexplored and this is the main reason why the experimental results of many researchers were over-predicted or under-predicted. Finally, the experimental data of single phase liquid flow through the microtubes under different conditions is very limited and experimental investigation is needed to clarify widely used LMTD method. Accordingly, numerical and analytic models proven by experimental results are very important in assessment of micro flow and heat transfer accurately. The main objectives of the current study are; (1) to investigate applicability of LMTD method for microscale heat transfer by experimental approach, (2) to compare flow and heat transfer characteristics with conventional theory and available results and (3) to show the scaling effects on heat transfer coefficients.

MATERIAL AND METHOD

A schematic of experimental apparatus is shown in Figure 1.a. The apparatus consists of a micro-pump, filter, fluid reservoir, heat exchanger, constant temperature bath, computer, data acquisition system and microtube test part. Deionized water was used in the current investigation as a working fluid. The fluid flow was supplied by the Gilson307 micro-pump (with damper module) in the range of 0.1–10 ml/min, and the pressurized tank was used to obtain higher volumetric flow rates. Two filters were placed the beginning micropump and after pressurized tank to prevent particles from entering the test tube.

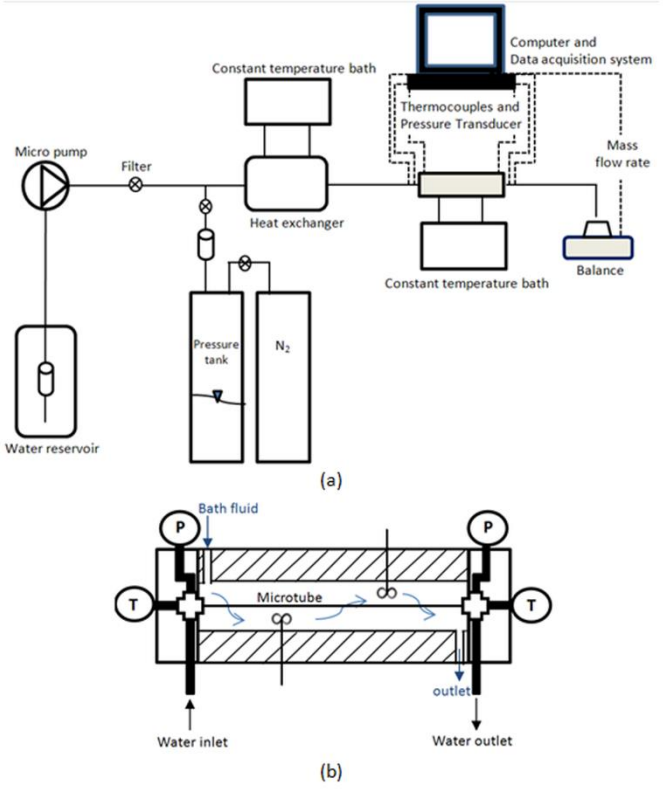

Figure 1. a) Experimental setup, b) Microtube test section

The water mass flow rate was determined by both from volumetric flow rate of the micro-pump and by the water mass collected per unit time on the balance on a digital balance (AND GX-600) during each test. As shown in Figure 1.b, the microtube connection ports, the two ends of the tested microtube, were specially fabricated from stainless steel to connect the tube. A single microtube was placed by connection ports in water jacked made of polymer material with low thermal conductivity. The out of test section is well insulated with glass wool leaving an air gap of 2–3 mm. Temperature of liquid bath was set and controlled by programmable constant temperature bath (Cole-Palmer

12108-25). Pressure transducer has been placed at microtube connection port and total pressure loss through the microtube was determined by measuring the pressure at the inlet with three different precision pressure transducers (Keller PA-33X 0–200 bar and 0–16 bar) which were chosen according the pressure level. The calibration of each electronic transducer has been checked before and after each of test run. The mean temperature of fluid was measured at both the entrance and the exit cross-section of the experimental set-up using K-type thermocouples placed in flow direction. All tests were conducted in a special test room whose temperature was precisely controlled. The temperature of the test room was adjusted based on the anticipated tube outer wall (outer surface of insulation) temperature so as to reduce the temperature difference between outer surface of the thermal insulation, and the temperature differences were checked periodically using a portable temperature measurement device. The measured data was collected after the time to be long enough to reach the steady conditions by a data acquisition system (Iotech Personal-Daq-3000). A data processing code was utilized for real-time calculations and monitoring the process. The difference between two successive measurements of the mass flow rate at any condition was generally negligible and within the experimental uncertainties. The fused silica tubes and stainless steel tubes were used (Ref. Parlak et al., [11]) and their specifications; diameters, lengths are listed in Table 1. The main problem was to precisely determine the average inner diameter of the microtube. The average inner diameter of a microtube could be determined by measuring the mass of microtube. Noting that the density of the tube material is known, one can calculate average diameter of the microtube by measuring its volume. Instead of this indirect method, we determined the average inner diameters at both ends of microtubes using a Scanning Electron Microscope (SEM, Vega Tescan) images. The images of area is scanned and calculated by a drawing program and then the average value is determined. A typical cross-section and the tube inside surface photos by a scanning electron microscope (SEM) are shown in Figures 2 a–b, respectively. In the study tests carried out, codes and Reynolds number ranges are listed in the Table 2.

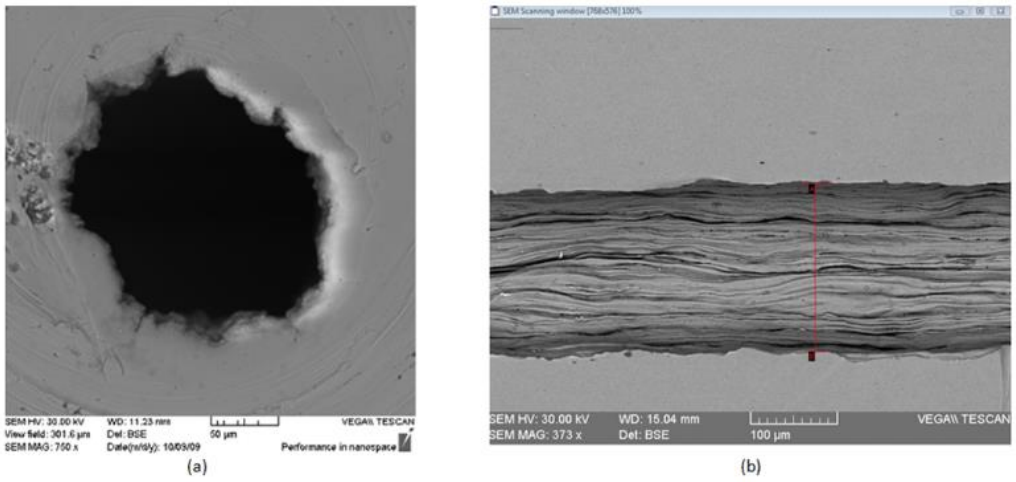

Figure 2. a) Stainless steel microtube, b) Stainless steel microtube

Table 1. Test tubes and specifications

Material	Diameter D (µm)	Error (±µm)	Roughness Є/D (%)	Dimensionless Length, L/D
Stainless steel	180	6.2	2.0-4.0	558
Stainless steel	180	6.1	2.0-4.0	1105
Stainless steel	180	6.2	2.0-4.0	1714
Stainless steel	103	10.7	4.0-6.0	971
Fused Silica	101	2.0	0	990

Table 2. Experiments and codes

Test Codes Material[Dimensionless Length] [Outer Temperature]	**Reynolds Range**	**Bath Temperature, °C** (Outer of Microtube)
SS[558][T=34]	100-4600	34.2-34.4
SS[1105][T=34]	100-4600	34.2-34.4
SS[1714][T=34]	100-1600	34.2-34.4
SS[1105][T=44]	100-1600	44.2-44.5
SS[1105][T=54]	100-1600	54.2-54.5
SS[1714][T=44]	100-1600	44.2-44.5
SS[1714][T=54]	100-1600	54.2-54.6
SS[558]	100-4600	Adiabatic
SS[971]	290-2600	Adiabatic
FS[990]	220-2400	Adiabatic

DATA REDUCTION

The Hagen-Poiseuille equation represents a functional relationship between volume flow rate and pressure loss in fully developed laminar flow. The pressure loss of flow through the tube can be calculated by;

$$\Delta P = 128 \frac{\mu L}{\pi D^4} \dot{V} \quad (4)$$

where μ, D, $\dot{V}$ are dynamic viscosity, inner diameter of microtube and volume flow rate, respectively. The average velocity U_m, for water flow in microtubes can be obtained from the mass flow rate measured in tests $\dot{m}$;

$$U_m = \frac{\dot{m}}{\rho A} \quad (5)$$

where A is the cross-sectional area of the micro tube, ρ is the fluid density. The Reynolds number is evaluated by

$$Re = \frac{\rho U_m D}{\mu} \quad (6)$$

In calculations, the fluid properties are evaluated at the fluid mean temperature, by averaging of inlet and outlet temperature and assumed to be independent of pressure. Finally, from Darcy's equation, the friction factor is given as;

$$f = \Delta P \frac{D}{L} \frac{2}{\rho {U_m}^2} \quad (7)$$

The heat transfer in steady-state operation with no heat losses and no phase changes can be calculated by the energy balance equation;

$$\dot{m} c_p (T_{in} - T_{out}) = UA\Delta T_m \quad (8)$$

where A denotes the heat transfer area (A = πDL) and U is the overall heat transfer coefficient can be calculated by;

$$\frac{1}{UA} = \frac{\Delta T_m}{\dot{m}c_p(T_{in}-T_{out})} = \frac{1}{h_i A_i} + \frac{ln(D_o/D_i)}{2\pi kL} + \frac{1}{h_o A_o} \quad (9)$$

T_{out}, T_{in} are the outlet and the inlet temperatures of fluid, respectively. ΔT_m is the logarithmic mean temperature difference between two fluids, determined from;

$$\Delta T_m \equiv \frac{(T_{o,o}-T_{in})-(T_{o,i}-T_{out})}{ln\frac{(T_{o,o}-T_{in})}{(T_{o,i}-T_{out})}} \quad (10)$$

The logarithmic mean temperature difference is an exact representation of the average temperature difference between hot and cold fluids and it reflects the exponential decay of the local temperature difference (Çengel [27]). In the typical heat exchanger analysis with the overall heat transfer coefficient the quantities of heat transfer coefficients particularly of fluid contact with the outer surface have to be known for exact solution. If the value of outer heat transfer coefficient is very high or the wall temperature is known, it can be neglected in the calculating of the inner heat transfer coefficient (Figure 3a). Based on the fact that the inner wall and local of fluid temperatures are immeasurable, an experimental method for determining heat transfer coefficient has been developed in the study. According to this method, there are three microtubes having same inner diameter but different lengths. One considers that there is no scale effect in the microtube and all tests are conducted under the same experimental conditions. The outlet temperatures of fluid through the all tubes are measured and the measured outlet temperature of fluid in short tubes can be accepted as the local temperature of fluid at the same distance from entrance of long tube. In this way, local temperatures of fluid through the microtube can be determined to compare with theoretical temperatures. Three microtubes scathed schematically with temperature details in Figure 3b. Also determining of the temperature inner surface of microtube wall, $T_{w,i}$, is very difficult by experimentally. In our experiments the temperature of water surrounding outer of microtube T_o is approximately ($\Delta T < 0.3$ ℃) kept constant. Water temperature is measured by K-type thermocouples at specified points at inner wall and also heat losses where connection parts are considered by the measured temperature.

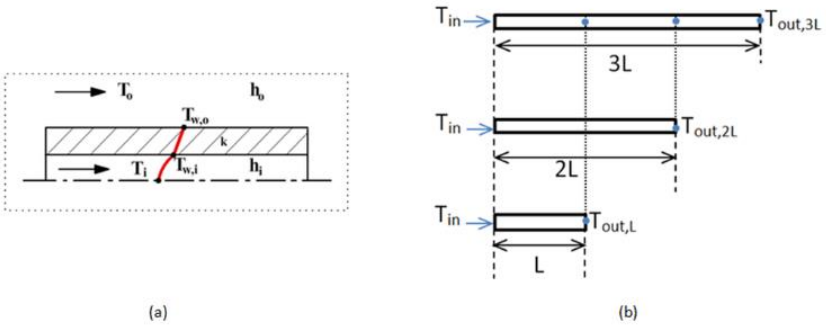

Figure 3. a) Temperatures on axial section of microtube, b) Experimental derivations with two shorter tubes for temperature distribution along the longer tube.

The inner wall temperatures ($T_{w,i}$), can be determined by heat conduction equation as follows;

$$T_{w,i} = T_{w,o} - \frac{Q_x\, ln(r_2/r_1)}{2\pi k L_x} \quad (11)$$

Where L_x is the tube length between microtube entrance and point where temperatures measured both outlet and wall. Also Q_x denote the enthalpy changes of the each microtube having different lengths. Finally the heat transfer coefficient by reducing of Eq. (9) with known inner wall temperature can be written as;

$$h_i = \frac{\dot{m}c_p(T_{in}-T_{out})}{\pi DL(T_{w,i}-T_m)} \quad (12)$$

and the Nusselt number,

$$Nu = \frac{h_i D}{k_f} \quad (13)$$

where k_f is the thermal conductivity of water calculated at the average fluid temperature.

Nu correlations for comparison

In the classical theory of internal laminar heat transfer, the Nusselt number for thermally fully developed flow is only dependent on the cross-sectional shape of the channel. Shah and London [28] found that the Nusselt number is between 4.36 and 3.66 for fully developed laminar circular pipe flow, which correspond to Nusselt numbers for constant heat flux and constant temperature boundary conditions, respectively. On the other hand, the average Nusselt number for simultaneously developing laminar flow in a circular tube (Re < 2300) can be determined from Sieder-Tate [29] equation;

$$Nu = 1.86\left(\frac{RePrD}{L}\right)^{1/3}\left(\frac{\mu_m}{\mu_s}\right)^{0.14} \quad (14)$$

All properties are evaluated at the mean fluid temperature, except for μ_s, which is evaluated at the surface temperature. Another correlation used in the comparison is Gnielinski [30] can be used in the transition from laminar to turbulent and turbulent regime for $3000 < Re < 5 .10^6$;

$$Nu = \frac{\left(\frac{f}{8}\right)(Re-1000)Pr}{1+12{,}7(f/2)^{\frac{1}{2}}(Pr^{\frac{2}{3}}-1)} \quad (15)$$

where

$$f = \frac{1}{(1{,}58lnRe-3.28)^2} \quad (16)$$

Table 3. Summaries of experimental studies and findings conducted in microchannels

Ref.	Correlations
Wang and Peng [12]	$\mathrm{Nu} = 0{,}0085\mathrm{Re}^{0.8}\mathrm{Pr}^{1/3}$
Tso and Mahulikar [5]	$\mathrm{Nu} = \mathrm{ARe}^{0{,}62}\mathrm{Pr}^{1/3}\mathrm{Br}^{0{,}165}$
Adams et al. [2]	$\mathrm{Nu}_{\mathrm{Gn}} = \frac{\left(\frac{\mathrm{f}}{8}\right)(\mathrm{Re}-1000)\mathrm{Pr}}{1+12{,}7\left(\frac{\mathrm{f}}{8}\right)^{\frac{1}{2}}\left(\mathrm{Pr}^{\frac{1}{3}}-1\right)}$
	$\mathrm{Nu} = \mathrm{Nu}_{\mathrm{Gn}}(1+\mathrm{F})$
Fernando et al. [16]	$\mathrm{Nu} = 4{,}526.10^{-4}\mathrm{Re}^{1.25}\mathrm{Pr}^{0.4}\left(\frac{\mu}{\mu_s}\right)^{0.14}$ for $2300 < \mathrm{Re} < 6000$

In addition, summary of the some experimental studies conducted in microchannels are demonstrated in the Table 3.

Uncertainty analysis

The classical method of Kline and McClintock [31] has been applied in order to estimate the uncertainty to be associated to the heat transfer coefficient values determined by means of Eq. (12). According to this approach, the uncertainty in a given function is due to the combined effects of uncertainty in all the variables, according to the well-known root-sum-square method. Standard uncertainties of some measured parameters, pressure drop, inlet temperature and flow rate are 0.3%, 0.6% and 0.6% and the maximum uncertainties are found 4.9%, 16.7% and 9.7 % for Re, f and Nu, respectively.

RESULTS AND DISCUSSION

The experiments have been conducted in the laminar flow range and friction factors were determined from the pressure drop using Darcy's equation (Eq. (7)). The theoretical laminar friction value (Hagen-Poiseuille) $64/\mathrm{Re}$ is also drawn in all the figures to compare the experimental results with the theoretical laminar flow characteristics. The results of the friction factor as a function of Reynolds number are presented in Figure 4. The measured friction factors for all tubes (particularly in smooth microtube) follows the theoretically line according to $64/\mathrm{Re}$ in the laminar flow regime. But as Re number increases, the measured friction factors of stainless steel tubes observed to be significantly higher than the values predicted by conventional theory, and the transition from laminar to turbulent flow starts at Re around 1500 for the smallest rough tube (103 μm ID). After value of Re=1500 it can be clearly seen that friction factors are found higher than predicted data of both 64/Re. In addition the critical Re numbers of the other rough tubes were found as 1900 for 179 μm ID. The reason for the early transition is that the internal surface and cross section of stainless steel tubes are not smooth and properly in contrast to fused silica tube.

Applicability of the LMTD method

The inner wall temperatures have been calculated by Eq. (11). The inner wall temperatures along the tube have been assumed to be constant since the difference between each other not exceeded the value of 0.5 ºC. Therefore the applicability of the logarithmic mean temperature difference method based on the constant wall temperature is discussed by experimental results.

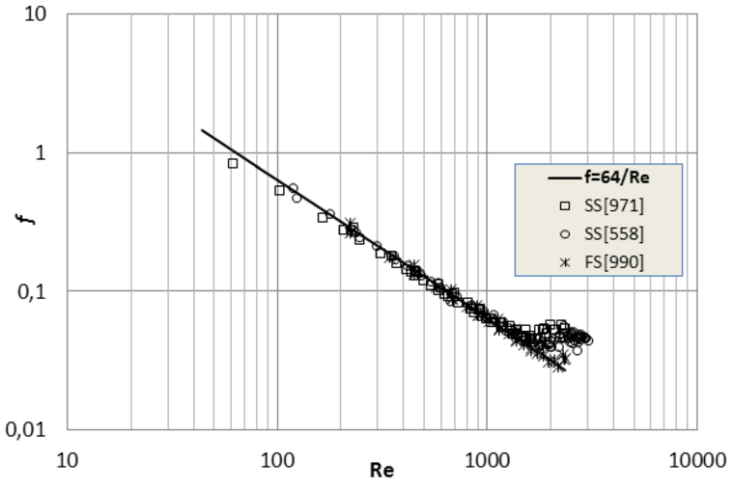

Figure 4. Measured friction factor versus Re number

The prediction local temperature of fluid can be calculated using constant heat transfer coefficient assuming that Nusselt number is equal to value of 3.66 with following equation reducing from Eqs. (9) and (10);

$$T_{out} = T_{w,i} - \left(T_{w,i} - T_{in}\right) exp\left(-\frac{(\pi D)L_x}{\dot{m}c_p} h_i\right) \quad (17)$$

and depicted as a function of L with straight line in Figure 5. The dashed line indicates experimental variation of fluid temperature determined using same equation (Eq. (17)) by approximation provided that values to be close to three measured outlet temperatures. For each volumetric flow rate, the method is applied and heat transfer coefficients are obtained for 10<Re<4500. Figures 5 a-d show variations of both calculated and measured temperatures with tube length in the laminar flow range. It is clearly seen that measurement data have not overlapped with values calculated theoretically (Nu=3.66). Otherwise the measured values were found to be compatible with a logarithmic curve computed by experimental heat transfer coefficient (Eq. (12)). This means that the measured data of outlet temperatures proves logarithmic behavior is valid. As volume flow rate increases, measured temperatures decrease and logarithmic curve gradually flattens as excepted. This method also applied to transitional flow range and results are presented in Figures 6 a-c.

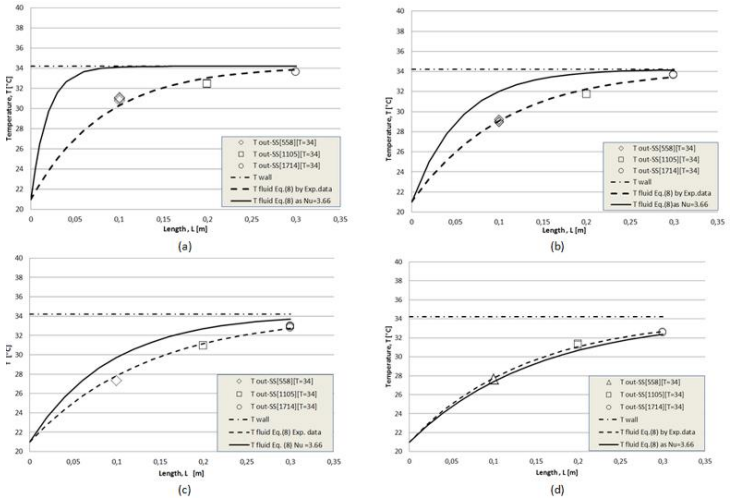

Figure 5. a) Comparison of measured temperatures with theoretical data at the same volumetric flow rate of 2 ml/min, b) for volumetric flow rate 6 ml/min, c) for volumetric flow rate 10 ml/min, d) for volumetric flow rate of 16 ml/min.

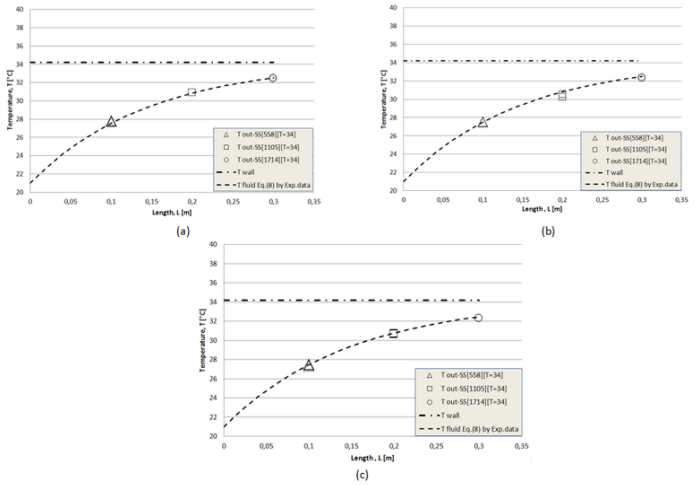

Figure 6. a) Comparing measured temperatures to theoretical data at same volumetric flow rate of 19 ml/min, b) for volumetric flow rate of 24 ml/min, c) for volumetric flow rate of 35 ml/min.

Also the measured temperatures are compatible with the temperature calculated logarithmic mean temperature method. Accordingly, the heat transfer coefficients are presented in Figure 7. The experimental results showed that the heat transfer coefficient increased with Re number both in transitional to turbulent and laminar flow region. The mean Nusselt numbers are obtained for Reynolds numbers in the range of 100-4500 to cover both laminer and transitional flow range. In order to perform an assessment of the experimental results by comparing with the heat transfer coefficient data from the literature for both conventional channel sizes and mini and microchannels, the Nu correlations are given in the open literature.

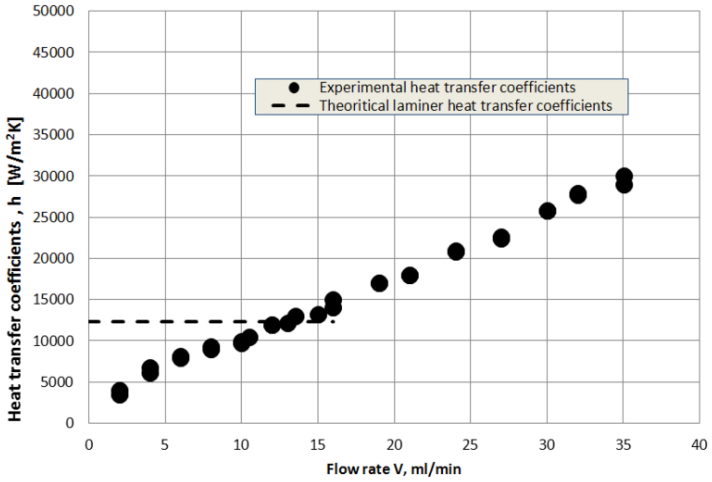

Figure 7. The variation of the experimental heat transfer coefficients with the Reynolds number

The measured Nusselt number increased with increasing Re at Reynolds range 280<Re<1400, but this increment became smaller for 1400< Re <1800. In Figure 8 the experimental results and correlations of Peng-Peterson [13], Wang and Peng [12], Adams et al. [2], Tso and Mahulikar [5], Fernando et al. [16], are compared with Edwards [32], Sieder-Tate [29], Gnielinski [30] correlations for an experiment with SS[1105][T=34]. In the laminar regime the correlations proposed by [13] and [5] are in disagreement with each other proposed for macro channels. Measured Nu numbers are found to be smaller than values obtained from existing correlations (by [32] and[29],) at Re < 2000, but the data is found to be closer to values obtained by Sieder-Tate correlations than the others. As the Reynolds number increases, measured Nusselt numbers increase with linear behavior. Deviations between the predictions and experiment are attributable mainly to experimental uncertainties. The results also indicate that the classical correlations at laminer and transitional flow are more applicable than some of the correlations which have been suggested for microchannels. Especially, in the laminar flow region, the experimental Nusselt numbers are in reasonably agreement with the Sieder-Tate correlation for thermally developing flow. Moreover predicted values from Gnielinski [30] and Adams [2], correlations remained lower than experimental data for Re>2000. It is seen that the predictions from correlations are seen to lie below the experimental data for Re>3400, possibly because the flow is not yet fully turbulent. After Re>3400, the values are relatively closer to the predictions of Adams [2] correlation. In the turbulent regime, the correlations of Wang and Peng [12] and Peng and Peterson [13] give lower Nusselt numbers than the Gnielinski correlations. Heat losses due to conduction through the test section ends were also estimated, and were found to be negligible.

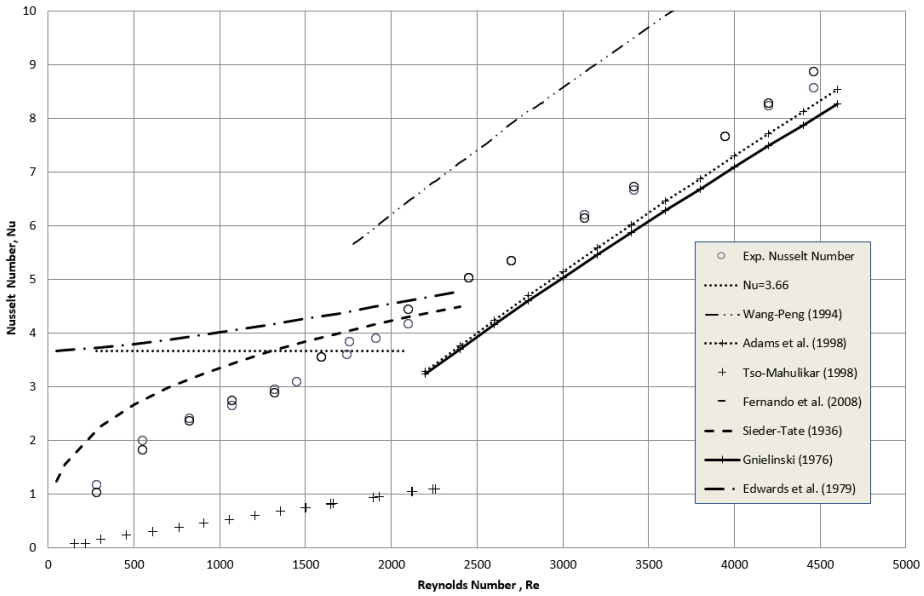

Figure 8. Variation of the experimental Nusselt numbers with the Reynolds number

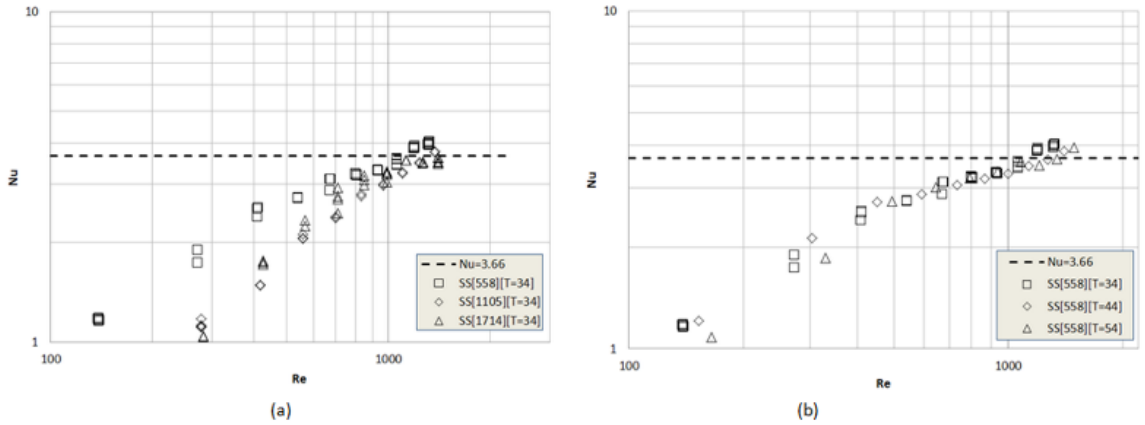

Figure 9. a) Experimental Nu numbers by Eq.(9) for three different tube lengths, b) Experimental Nu numbers at different wall temperatures (by Eq.(9))

In thermally fully developed laminar flow Nusselt number equals to the value of 3.66 for constant temperature boundary conditions. The Nusselt numbers obtained at laminar region (especially Re<1500) are found to be smaller than theoretical values as seen Figure 8. The first reason of that is incalculable heat losses. Under heating conditions, test section walls are covered to avoid heat losses, which have been explained in material and method section. In low Reynolds number, incalculable heat losses would never effect if tubes was conventional size. But in microtubes experiments, these heat losses reduced total heat transfers and caused heat transfer coefficients approximately were up to 25% lower than predicted. On the other hand, in the experimental studies on microchannels, geometries and measured mass flow rate considerably smaller than conventional channels, and their uncertainties effect on calculated values. These results suggest that the scaling effects such as axial conduction, viscous heating, entrance effect, wall roughness and are taken into consideration to make an accurate assessment. The first possible effect plays important role in the heat transfer is the entrance effect. The heat transfer coefficients are calculated in all tubes by Eq.(12) and the results obtained from short tubes are compared to longer tubes for making assessment of scaling effects. The corresponding average Nusselt number is calculated as $Nu = hD/k$ in which the thermal conductivity of water was

evaluated at the average fluid temperature. Figure 9 shows the variation of the experimentally obtained Nusselt numbers as a function of Reynolds numbers for the three different tube diameters. Nusselt numbers for the shortest tube are found to be greater (up to 30% in average) than the others. As thermal entrance lengths compared to the total length of tubes, the highest value (≈ 60%) is in short microtube with length of 10 cm at laminar flow range and the Graetz number varies from 10 to 23.4 when Reynolds number varies from 900 to 2100. This means that the flow is not thermally fully developed flow (Gz>10). When the length of tube increases, the thermal entrance effect is reduced and results obtained from longer tubes (20 and 30 cm) overlap with each other.

Another important issue is the heat losses particularly in places where temperatures measured cannot be prevented and causes to differences in experimental results. If the heat losses are not taken into account in calculations, heat transfer coefficients may be as shown found smaller than that it has been. This effect can be seen in particular at low Re number Re<350 as shown Figure 9b. When the temperature difference between test bath and room is high, the heat loss will increase and h will reduce at the highest wall temperature (54 ºC). Because of making the experimental method explained in section material and method was applied to minimize the effect of heat losses. In addition the criterion proposed by Maranzara [23] (Eq. (2)) is used to determine whether axial conduction effects have to be taken into account. The axial conduction in the wall can be neglected when the non-dimensional number M gets lower than 0.01. Since experiments are conducted at Reynolds number range of 200 to 4500, the value of M will exceed 0.01 and heat transfer by conduction along the walls of microtubes is not considered in the present study. Variations of the cross-section geometry and the roughness are the two major effects on Nu number. Since these variations are always within the limits of experimental uncertainties, in the study the roughness effect are not considered. For heating regimes two factors which are convective heat transfer and heat released due to viscous dissipation determine the temperature distribution of the fluid. The heat transferred from wall to the cold fluid and the heat released due to viscous dissipation both lead to increase in fluid temperature. As the temperature difference between fluid and wall increases, the Br number decrease at the same Reynolds number. Increasing the Br numbers in the experiments mean that Nu numbers are lower than that actual values according to correlation of $Nu = Nu_0 - 8Br$. Also the ratio of κ between the temperature rises related to the viscous heating and the heat flux at the walls came down as the temperature difference was high and at the opposite case became important. Our experimental Br numbers were found to vary between $3.98.10^{-5}$ and 0.09 within Reynolds ranges of 138~4880 respectively. For Re>800 the viscous heating became significant and to show the effect on the Nu number, Nu number versus Br number plotted in the Figure 10 disregarding the effect of Re number. Figure shows that the measured Nu numbers decreased as Br numbers increased at the same Reynolds number. As mentioned in the previous section the mean Nu numbers increased with the Re number in the laminar flow region. Only in the range of Reynolds number 1300-1700 the mean Nu numbers compatible with the data obtained by correlation of $Nu = Nu_0 - 8Br$. In this Reynolds range the viscous heating effect on Nu number was an average of 9%.

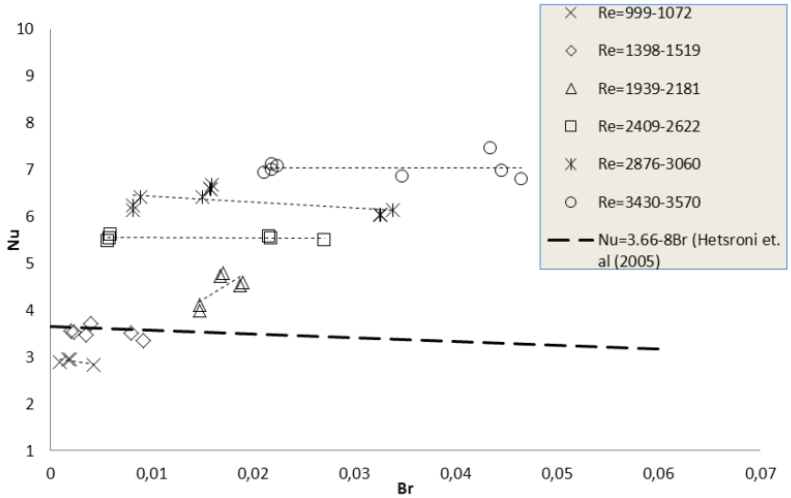

Figure 10. Variation experimental Nu number with Br number

CONCLUSION

In the present study, the applicability of the logarithmic mean temperature difference method based on the constant wall temperature is discussed by experimental results. The heat transfer coefficients of water flow through the single microtube in a bath set constant temperature are found experimentally. The measured heat transfer coefficients in laminar flow in stainless steel tubes have exhibited a Reynolds number dependence. The Nusselt number increases with increasing Reynolds number and do not accord with the conventional results when Reynolds number is lower than 1000 and after than Nusselt number approached the conventional laminar theory prediction. Also the results indicated that the measured temperatures were compatible with a logarithmic curve computed by experimental heat transfer coefficient and confirmed that the logarithmic behavior was valid. Experimental friction factors are obtained for deionized water flowing in stainless steel and fused silica microtubes. The measured friction factors are found to be compatible with the data obtained from theoretical correlation (64/Re) in the laminar flow region. But for higher Re numbers, the measured friction factors of stainless steel tubes are significantly higher than the values predicted by conventional theory and the transition from laminar to turbulent flow starts at Re around 1500 at smallest rough tube (103 μm ID). In addition, the scaling effects have been considered and results have been compared with data obtained by the available correlations. Results showed that the axial conduction in the fluid and wall was not affect the heat transfer in microtubes for Re>140. For Re>800 the viscous heating became significant and to show the effect on the Nu number and the measured Nu numbers decreased as Br numbers increased.

ACKNOWLEDGMENTS

The authors are thankful for the funding provided by the State Planning Organization of Turkey under Grant No. 2003-K-120-970.

NOMENCLATURE

A	area (m^2)
Br	Brinkman number
c	specific heat ($J \cdot kg^{-1} \cdot K^{-1}$)
D	inner diameter (μm)
e	roughness height (m)
f	Darcy friction factor
Gr	Graetz number
H	micro-channel height (m)
h	heat transfer coefficient
k	thermal conductivity ($W.\ m^{-1}.K^{-1}$)
L	length of tube (m)
M	Axial heat conduction ratio (-)
$\dot{m}$	mass flow rate ($kg \cdot s^{-1}$)
Nu	Nusselt number
P	absolute pressure (Pa)
Pe	Peclect number
Pr	Prandtl number
Re	Reynolds number
Q	Heat transfer ($kJ \cdot s^{-1}$)
T	temperature (K)
ΔT	temperature increase (K)
U	Overall heat transfer coefficient ($W \cdot m^{-2}.K^{-1}$)
U_m	mean velocity of fluid ($m \cdot s^{-1}$)
$\dot{V}$	volumetric flow rate ($m^3 \cdot s^{-1}$)
W	micro-channel weight (m)

Greek symbols

κ	Viscous heating ratio (-)
μ	fluid viscosity ($N \cdot s \cdot m^{-2}$)
ρ	Density (kg. m^{-3})

Subscripts

c	cross section
exp	experimental
f	fluid
gen	generation
h	hydraulic
i	inner
in	inlet
L	laminer
m	mean
o	outer
out	outlet
q	heat
ref	reference
s	surface
T	turbulent
th	theoretical
v	viscous
w	wall

REFERENCES

[1] Kandlikar S.G., Heat Transfer and Fluid Flow in Minichannels and Microchannels (Second Edition), Chapter 3, Single-Phase Liquid Flow in Minichannels and Microchannels, Pages 103–174, 2014.

[2] Adams T M, Abdel-Khalik S I, Jeter S. M, Qureshi Z H. (1998) An experimental investigation of single-phase forced convection in microchannels. Int J Heat Mass Transfer; 41: (6–7) 851–857.

[3] Yu D, Warrington R, Barron R, Ameel T. (1995) An experimental investigation of fluid flow and heat transfer in microtubes. Proceedings of the ASME/JSME Thermal Engineering Conference, Vol. 1. American Society of Mechanical Engineers, pp. 523-530.

[4] Celata G P, Cumo M, Guglielmi M, Zummo G. (2002) Experimental investigation of hydraulic and single phase heat transfer in 0.130 μm capillary tube. MicroscaleThermophys Eng; 6: 85–97.

[5] Tso C P, Mahulikar S P, (1998) The use of Brinkman number for single phase forced convective heat transfer in microchannels. Int J Heat Mass Transf; 41: 1759-1769.

[6] Lelea D, Nishio S, Takano K. (2004) The experimental research on microtube heat transfer and fluid flow of distilled water. Int J Heat Mass Transfer; 47: 2817–2830.

[7] Celata G P, Morini G L, Marconi V, McPhail S J, Zummo G. (2006) Using viscous heating to determine the friction factor in microchannels – An experimental validation. Experimental Thermal and Fluid Science; 30: 725–731.

[8] Li Z, He Y L, Tang G H, Tao W Q. (2007) Experimental and numerical studies of liquid flow and heat transfer in microtubes. Int J Heat Mass Transfer; 50: 3447–3460.

[9] Zhigang L, Ning G, Chengwu Z, Xiaobao Z. (2009) Experimental study on flow and heat transfer in a 19.6 μm microtube. Experimental Heat Transfer; 22: 178-197.

[10] Parlak N, Gür M, Arı V, Küçük H, Engin T. (2010) Second law analysis of water flow through smooth microtubes under adiabatic conditions. Experimental Thermal and Fluid Science; 35: 60-67.

[11] Parlak N, Gür M, Arı V, Küçük H, Engin T. Mikroborularda ısı geçişinin deneysel incelenmesi. ULIBTK'11 18. Ulusal Isı Bilimi ve Tekniği Kongresi, 07-10 Eylül 2011, Zonguldak.

[12] Wang B and Peng X. (1994) Experimental investigation on liquid forced-convection heat transfer through microchannels. Int J of Heat Mass Transfer; 31: 73-82.
[13] Peng X F and Peterson G P. (1996) Convective heat transfer and friction for water flow in micro-channel structures. Int J Heat Mass Transfer; 39: 2599–2608.
[14] Harms T M, Kazmierczak M J, Gerner F M. (1996) Developing convective heat transfer in deep rectangular microchannels. Int J Heat Fluid Flow; 20: 149–157.
[15] Gao P, Le Person S, Favre-Marine M. (2002) Scale effect on hydrodynamics and heat transfer in two-dimensional mini and microchannels. Int J Thermal Sciences; 41: 1017-1027.
[16] Fernando P, Palm P, Ameel T, Lundqvıst P, Granryd E. (2008) A minichannel aluminium tube heat exchanger – Part I: Evaluation of single-phase heat transfer coefficients by the Wilson plot method. Int. J. of Refrigeration; 31: 669-680.
[17] Lee P S, Garimella S V, Liu D. (2005) Investigation of heat transfer in rectangular microchannels. Int J HeatMassTransfer : 48; 1688-1704.
[18] Qu W, Mala M, Li D. (2000) Heat transfer for water flow in trapezoidal silicon microchannels. Int J HeatMass Transfer; 43: 3925-3936.
[19] Wu H Y, Cheng P. (2003) An experimental study of convective heat transfer in silicon microchannels with different surface conditions. Int J Mass Transfer; 46: 2547–2556.
[20] Tiselj I, Hetsroni G, Mavko B, Mosyak A, Pogrebnyak E, Segal Z. (2004) Effect of axial conduction on the heat transfer in micro-channels. Int J Heat Mass Transfer; 47: 2551–2565.
[21] Hetsroni G, Mosyak A, Pogrebnyak E, Yarin L P. (2005) Heat transfer in micro-channels: Comparison of experiments with theory and numerical results. Int J Heat Mass Transfer; 48: 5580–5601.
[22] Morini G L, Lorenzini M, Salvigni S, Celata G P. (2010) Experimental analysis of microconvective heat transfer in the laminar and transitional regions. Experimental Heat Transfer; 23: 73–93.
[23] Maranzana G, Perry I, Maillet D. (2004) Mini- and micro-channels: influence of axial conduction in the walls. Int J Heat Mass Transfer; 47: 3993–4004.
[24] Kandlikar S G, Joshi S, Tian S. (2003) Effect of surface roughness on heat transfer and fluid flow characteristics at low Reynolds numbers in small diameter tubes. Heat Transfer Engineering; 24: 4-16.
[25] Kandlikar S G, (2005) Roughness effects at microscale – reassessing Nikuradse's experiments on liquid flow in rough tubes. Bull Pol.Acad.Technol; 53: 343–349.
[26] Asadi M., (2014) A review of heat transfer and pressure drop characteristics of single and two-phase microchannels, International Journal of Heat and Mass Transfer, Vol. 79, Pages 34–53.
[27] Cengel Y A. Heat Transfer: A Practical Approach. New York, USA: McGrawHill, 2003.
[28] Shah R, London A. Laminar Flow Forced Convection in Ducts. New York, USA; Academic Press, 1978.
[29] Sieder E N and Tate G E. (1936) Heat transfer and pressure drop of liquids in tubes. Industrial Engineering Chemistry; 28: 1429-1435.
[30] Gnielinski V. (1976) New equations for heat transfer in turbulent pipe and channel flow. Int Chem Eng; 16: 359–368.
[31] Kline S J and McClintock F A. (1993) Describing uncertainties in single-sample experiments. Mech Eng;75;3–8.
[32] Edwards D K, Denny V E, Mills A F. Transfer Processes. Washington, DC: Hemisphere, 1979.